NANO LETTERS

Letter

pubs.acs.org/NanoLett

Coupling Two Distant Double Quantum Dots with a Microwave Resonator

Guang-Wei Deng,[†,‡] Da Wei,[†,‡] Shu-Xiao Li,[†,‡] J. R. Johansson,[§] Wei-Cheng Kong,[†,‡] Hai-Ou Li,[†,‡] Gang Cao,[†,‡] Ming Xiao,[†,‡] Guang-Can Guo,[†,‡] Franco Nori,[∥,⊥] Hong-Wen Jiang,[#] and Guo-Ping Guo*[,†,‡]

[†]Key Laboratory of Quantum Information, University of Science and Technology of China, Chinese Academy of Sciences, Hefei 230026, China

[‡]Synergetic Innovation Center of Quantum Information and Quantum Physics, University of Science and Technology of China, Hefei, Anhui 230026, China

[§]iTHES Research Group and [∥]CEMS, RIKEN, Wako-shi, Saitama, 351-0198, Japan

[⊥]Physics Department, The University of Michigan, Ann Arbor, Michigan 48109-1040, United States

[#]Department of Physics and Astronomy, University of California at Los Angeles, Los Angeles, California 90095, United States

Supporting Information

ABSTRACT: We fabricated a hybrid device with two distant graphene double quantum dots (DQDs) and a microwave resonator. A nonlinear response is observed in the resonator reflection amplitude when the two DQDs are jointly tuned to the vicinity of the degeneracy points. This observation can be well fitted by the Tavis−Cummings (T−C) model which describes two two-level systems coupling with one photonic field. Furthermore, the correlation between the DC currents in the two DQDs is studied. A nonzero cross-current correlation is observed which has been theoretically predicted to be an important sign of nonlocal coupling between two distant systems. Our results explore T−C physics in electronic transport and also contribute to the study of nonlocal transport and future implementations of remote electronic entanglement.

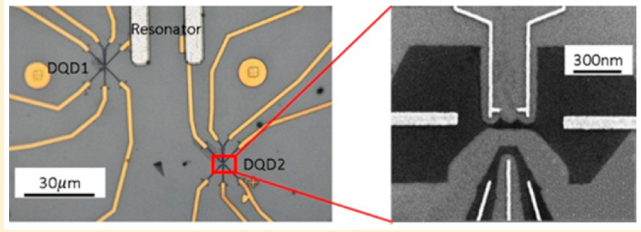

KEYWORDS: *Graphene, double quantum dot, resonator, cross-correlation, microwave*

Coupling distant nanoconductors is an important goal for nanophysics and for its potential applications. This kind of coupling needs the study of interaction between atoms and photons, which has been widely studied in cavity QED,[1] and circuit QED has extended this idea to on-chip superconducting qubits.[2−4] Recent theoretical[5−12] and experimental[13−22] studies have also implemented this architecture with quantum dots by coupling them to resonators. So far, resonators have been coupled to quantum dots made of GaAs,[14,16] carbon nanotubes,[13,17,19,22] InAs nanowires,[15,20,21] and graphene.[18] Beyond that, photon-mediated distant coupling between two single quantum dots (SQDs) has been studied.[17] Recently, in theoretical work on DQDs interacting through resonators, it has been proposed that this setup can be used to entangle macroscopically separated electron transport, which has applications in nanoscale quantum information processing and Bell inequality tests.[9−12] A first step toward these goals would be an experimental demonstration of photon-mediated nonlocal electronic transport effects in separated mesoscopic quantum systems.[11]

In general, the energy-level splitting in a DQD is easier to tune than in a SQD. In a DQD, the energy splitting can be directly controlled through the gate-induced detuning and can be tuned to an energy scale that is close to that of the resonator photons. Motivated by this, we here use DQDs to investigate the dispersive DQD-resonator coupling near the charge-degeneracy points of the two DQDs. We report an experimental demonstration of coupling, through a microwave resonator, between two distant DQDs which are separated by about 60 μm. When sweeping the detuning of each DQD, in the proximity of the charge-degeneracy points, a dip is observed in the resonator reflection amplitude due to nonadditive dispersive contributions from the two DQDs. This phenomenon is explained by the Tavis−Cummings model,[23] and it demonstrates the simultaneous dispersive coupling between one photonic mode and two DQDs. Moreover, with finite-bias voltages, the current through one of the DQDs is affected by the current through the other. By changing the microwave power applied to the resonator, this interaction can be controlled. Moreover, with finite-bias voltages, the cross-current correlation between the two DQDs is measured, and a positive correlation is found. This correlation between currents is studied with one DQD dispersively coupled to the resonator,

Received: June 17, 2015
Revised: August 28, 2015
Published: September 1, 2015

DOI: 10.1021/acs.nanolett.5b02400
Nano Lett. 2015, 15, 6620−6625

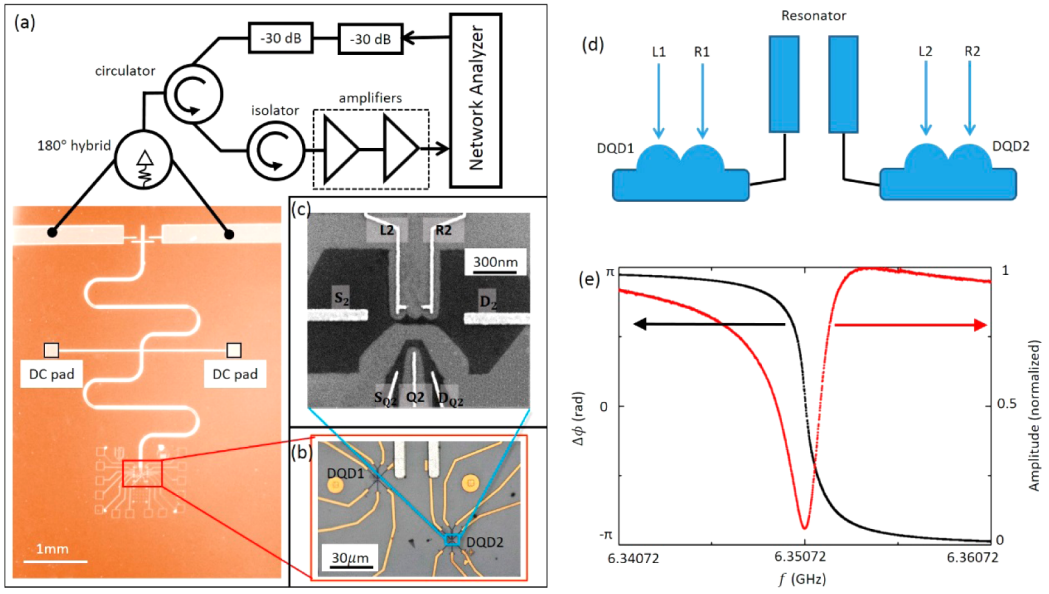

Figure 1. (a) Schematic and micrograph of the hybrid device. The half-wavelength reflection-line resonator is connected to the two DQDs at one end of its two striplines, while the other end is used for microwave input and output. (b) The two DQDs are separated about 60 μm and are each coupled to one stripline respectively through their source leads. (c) Scanning electron micrograph of a typical etched graphene DQD sample. (d) Schematic diagram of the hybrid device. The electric potentials of DQD1(2) L1(2) and R1(2) gates. (e) Spectrum of the phase (black) and amplitude (red) response of the reflection-line resonator with both DQDs in the blockade region, from which we extract the resonance frequency f_0 = 6.35086 GHz, internal loss $\kappa_{int}/2\pi$ = 0.68 MHz, and external loss $\kappa_{ext}/2\pi$ = 1.32 MHz.

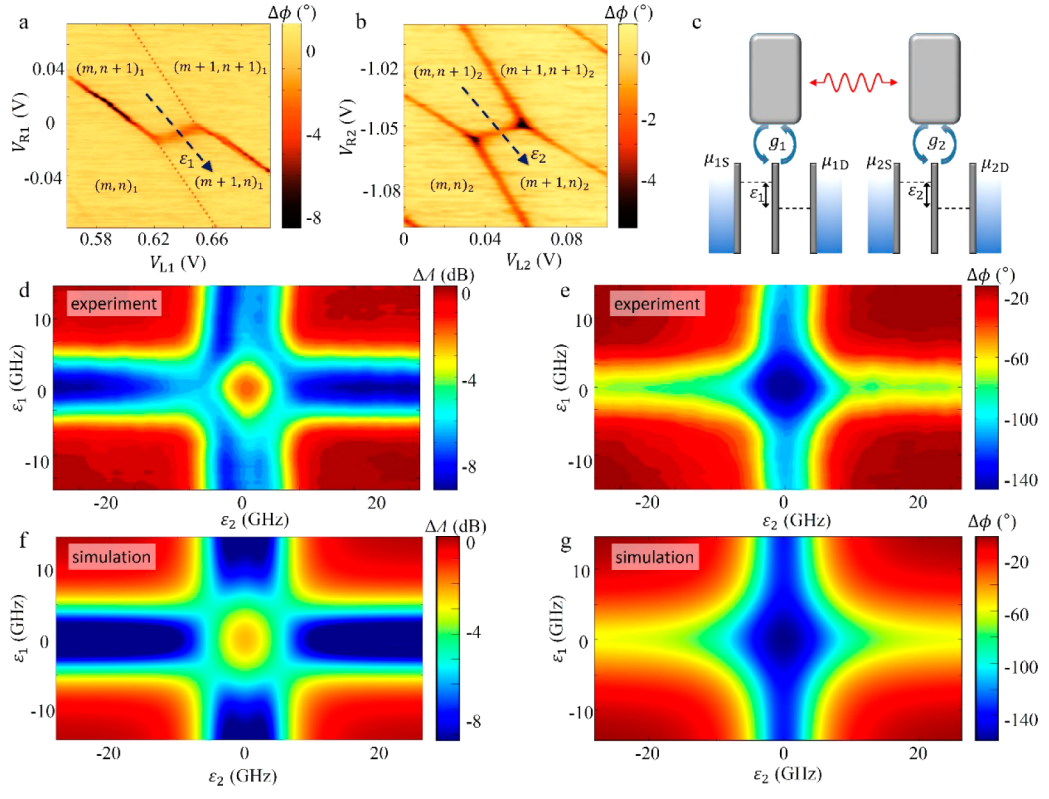

Figure 2. (a–b) Phase response of the resonator versus gate voltage near the (M + 1, N) ↔ (M, N + 1) charge transition for the two DQDs (a for DQD1 and b for DQD2), measured at a fixed probe frequency, f_R = 6.35200 GHz. The dashed arrows indicate the DQD energy detuning (ε_1 and ε_2) axes. (c) Schematic diagram of the coupling process. The DQDs are coupled to the resonator with coupling strengths g_1 and g_2 respectively. Microwave photons are confined between two isolated superconductors, inducing an interaction between the two DQDs without direct tunneling, or capacitive coupling between them. (d–g) Experimental (d–e) and simulated (f–g) results for the amplitude (d and f) and phase (e and g) response versus the detuning of each DQD. Parameters used in the simulation are taken from the best fits of the phase response versus detuning of each DQD, as denoted in a and b.

DOI: 10.1021/acs.nanolett.5b02400
Nano Lett. 2015, 15, 6620–6625

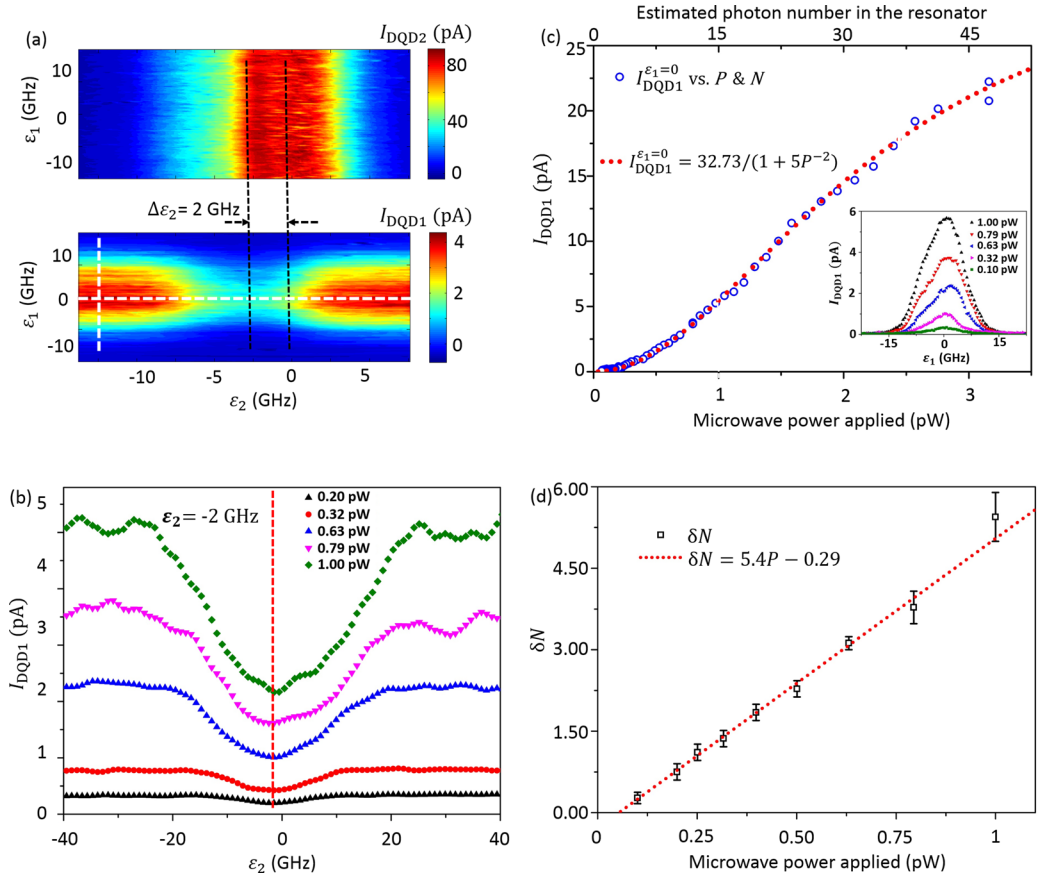

Figure 3. (a) DC current through DQD2 and DQD1 versus the two DQDs' detuning, ε_1 and ε_2. The microwave power resonantly applied to the resonator is about 0.79 pW. (b) I_{DQD1} versus ε_2, with different input microwave powers. All curves can be seen as cuts at the horizontal dashed white line in a, fixing $\varepsilon_1 = 0$. (c) Current peak of DQD1 versus microwave power P, obtained from the vertical dashed white line in a. Red dotted line shows the best fit of the obtained data. The inset diagram displays I_{DQD1} versus ε_1, with different microwave powers. (d) Photon number variation δN due to DQD2 being on and off resonance, versus microwave applied to the resonator, obtained from the current variations shown in b and the photon number-current relation shown in c.

while the coupling between the other DQD and the resonator can be tuned from dispersive to resonant.

Results and Discussion. Our sample is mounted in a dry dilution refrigerator, with a base temperature of about 38 mK. The resonator has a fundamental frequency f_0 of about 6.35086 GHz and a quality factor of about 3100. The hybrid device is shown in Figure 1. Two etched graphene DQDs,[24,25] made of separated (about 60 μm) few-layer flakes, are coupled to a superconducting reflection-line resonator[18,26,27] (RLR) through their sources (Figure 1b). From the obtained honeycomb and Coulomb diamond diagrams, we characterize the DQDs by their charging energies and lever arms (see Supporting Information). Meanwhile, charge-stability diagrams of both DQDs can also be obtained via the dispersive readout of the resonator (Figure 2a,b). Using the method described in ref 18, we further characterize the device. The DQD-resonator coupling strength g_{Ci}, the tunnel coupling strength $2t_{Ci}$, and dephasing rate γ_{2i} for the ith DQD are obtained.

Compared to the SQD charging energy,[24] $E_c \approx 2$ meV, the energy scale $2t_C$ is much closer to the resonator photon energy,[25] $hf_0 \approx 27$ μeV. Thus, we expect that the DQDs can interact via the resonator, when both DQDs have $2t_C$ comparable to hf_0 and are operated near their charge-degeneracy points. First, we tune the two DQDs to the proximity of interdot charge transition lines that correspond to near-6-GHz tunnel coupling. Next, we sweep the detunings (each along the dashed arrows, shown in Figure 2a,b) and record the resonator signal. Figure 2d,e show the experimental results under a 0.10 pW (−100 dBm) applied microwave power. Near the center (corresponding to the charge-degeneracy points of both DQDs) the reflection amplitude is distinctly different from other regions, in that the contributions of the two DQDs are nonadditive.

This observation matches well with the results of the T−C model[23] with the Hamiltonian:

$$H = \omega_0 a^\dagger a + \sum_{i=1,2}\left[\frac{1}{2}\Omega_i\sigma_{zi} + g_i(\sigma_{+i}a + \sigma_{-i}a^\dagger)\right]$$

where $g_i = g_{Ci}(2t_{Ci}/\Omega_i)$, $\Omega_i = ((2t_{Ci})^2 + \varepsilon_i^2)^{1/2}$. Here ω_0 is the resonance frequency of the resonator, and ε_i denotes the detuning of DQDi. This model describes two two-level systems that are coupled to a photonic field. Using this model with the obtained parameters (see Supporting Information), we can reproduce the experimental amplitude and phase diagram (Figure 2f,g). The tunnel coupling strengths for both DQDs are 7.2 GHz, and the DQDs are therefore in the dispersive regime ($\Omega_i - hf_0 \gg g_i$).

We can understand this phenomenon as follows. Since the two DQDs are coupled to the resonator, they can both cause frequency shifts. Particularly, when the DQDs have zero detuning, they both significantly contribute to the dispersive

DOI: 10.1021/acs.nanolett.5b02400
Nano Lett. 2015, 15, 6620−6625

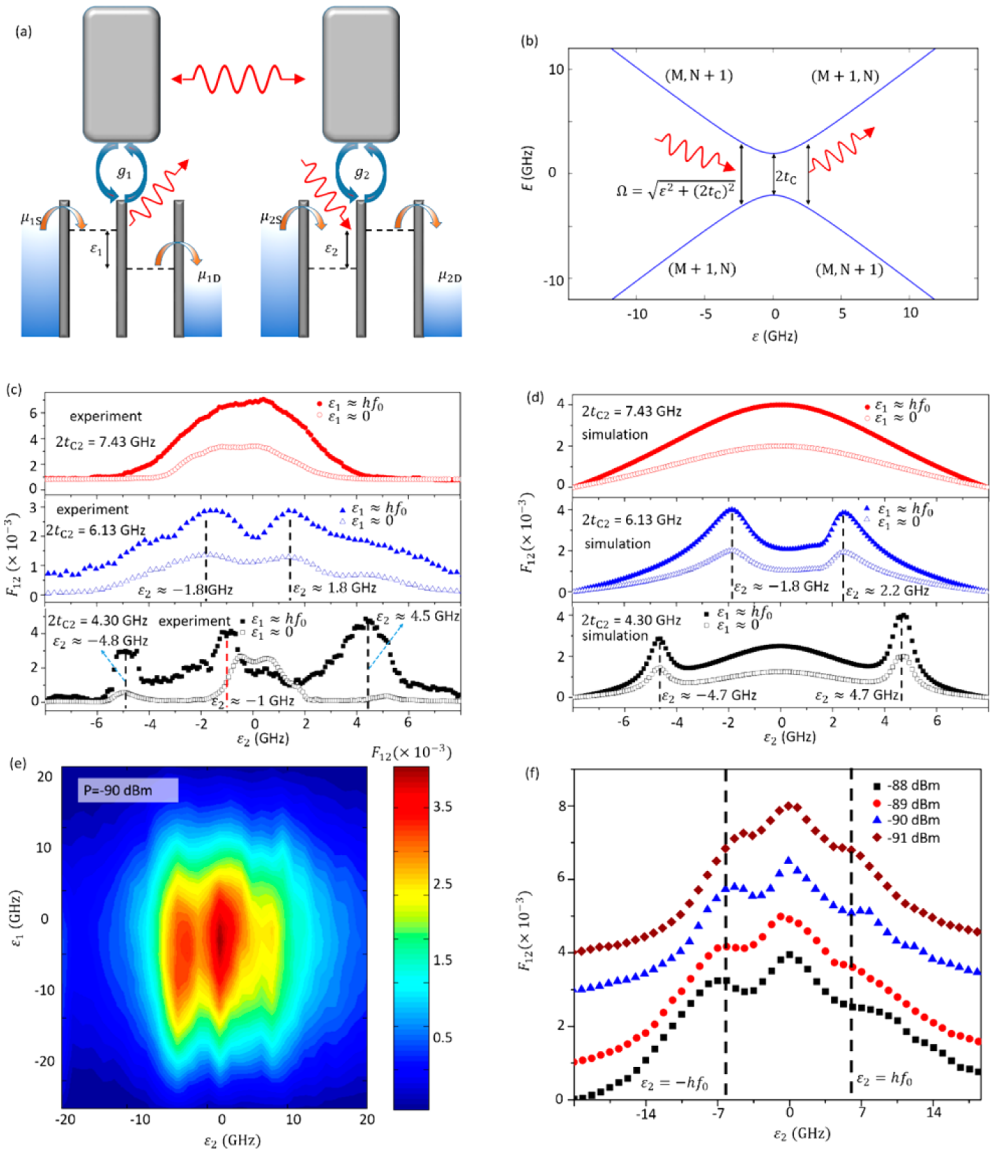

Figure 4. (a) Schematic diagram of the interaction mechanism. The two DQDs are biased at V_{SD1} = 500 μV and V_{SD2} = 500 μV. The resonator is not driving in this case. (b) Energy levels of a typical DQD versus detuning ε. (c) Normalized zero-frequency component of the cross-current spectrum F_{12}, as a function of detuning ε_2 with different interdot tunnel rates corresponding to different triple points, for two ε_1 values. (d) Simulation results for F_{12}, the peak positions are mostly consistent with the experimental data. (e) F_{12} as a function of the detuning of the two DQDs, with −90 dBm driving power. (f) Cut-off from part e with several driving powers. The peak positions are $\varepsilon_2 = -hf_0$, 0, and hf_0. The F_{12} can be converted to the noise power spectrum density by a factor of 10^{-24} A^2/Hz (see the Supporting Information).

interaction. These contributions add linearly, however, the amplitude and phase shifts of the resonator response are nonlinear. In other words, as shown in Figure 2d, instead of reaching a larger amplitude shift (of greater absolute value), the cross-center region have a far lower one, as if the two shifts compete with and cancel out each other. This is a natural result of the T−C model and can be reproduced in simulations. However, limited by the large dephasing rates in DQD systems, vacuum Rabi splitting and energy anticrossings[2,28] have not been observed in our device, restricting us from further exploring its quantum information applications. However, this DQD-resonator system described by the T−C model leaves us with opportunities to study interesting aspects of nonlocal electronic transport properties, which have been studied by theoretical works.[9−12]

Inspired by these predictions, we repeated the gate-sweeping procedures of the joint readout, but with focus on the DC current signals $I_{DQD1(2)}$ instead. Unless stated otherwise, the bias voltage is 60 μV for both DQDs throughout this part of the experiment. The DQDs are tuned to sites where $2t_{C1} > hf_0$ while $2t_{C2} \approx 6.1$ GHz $< hf_0$. Figure 3a shows I_{DQD1} and I_{DQD2} as a function of ε_1 and ε_2. I_{DQD1} decreases the most when $\varepsilon_2 = -2$ GHz, where DQD2 is in resonance with the resonator photon, i.e., $hf_0 = \Omega_2 = (\varepsilon_2^2 + (2t_{C2})^2)^{1/2}$. Fixing ε_1 at zero, we sweep ε_2 (shown as the horizontal white dashed line in Figure 3a) under a series of microwave powers. The result indicates that I_{DQD1} is influenced by DQD2 (Figure 3b). Furthermore, if we view DQD2 as a switch whose on and off states denote whether DQD2 is on resonance ($\Omega_2 \sim hf_0$) or off resonance ($\Omega_2 \gg hf_0$) with the resonator, such a switch is able to control the resonator photonic field strength. From Figure 3b, one can

DOI: 10.1021/acs.nanolett.5b02400
Nano Lett. 2015, 15, 6620−6625

extract the difference in I_{DQD1}, δI, for when DQD2 is on and off resonance. By converting δI into a difference in the average photon number δN, we can study DQD2's effect on the photonic field strength in the resonator (i.e., the average photon number N). To this end, we first employ the empirical law $I_{DQD1}^{\varepsilon_1=0} = 32.73/(1 + 5P^{-2})$ as shown in Figure 3c, with the current in units of pA and power in pW. One pW (−90 dBm) of applied power corresponds to about 5×10^4 photons in the resonator of our device, when both DQDs are in the Coulomb blockade regimes. Thus, when DQD2 is in the blockade regime, $I_{DQD1}^{\varepsilon_1=0}$ as a function of N can be approximated as $I_{DQD1}^{\varepsilon_1=0} = 32.73/(1 + 2 \times 10^{-9}\ N^{-2})$. The microwave response of the current through quantum dots has been studied previously, theoretically via the quantum photovoltaic effect in DQDs,[29] experimentally in the microwave response of a SQD made of GaAs,[30] and in the photon-induced current in graphene QDs at visible wavelengths.[31] The current−power relation we obtained above can be explained as electron heating by the resonator microwave field. As Figure 3d indicates, we find that δN depends linearly on P and thus on N. A physical consequence of this linear relation is that, in this power range, the total photon number in the resonator changes by a constant factor (∼36%) when DQD2 is on and off resonance.

The above observed phenomenon, caused by thermal effect, cannot be used to couple quantum information between the two DQDs. To study the quantum correlations between the currents in the two DQDs, we measure the zero-frequency component of the cross-current spectrum through a measurement of $S_{12}(0) = \langle \mathrm{FFT}^*(I_{DQD1})\mathrm{FFT}(I_{DQD2})\rangle$ using a dynamic signal analyzer (DSA). The machine, SR785, has been used to sensitively measure the charge noise of an undoped GaAs DQD[32] and a suspending graphene QD[33] in our lab. A fixed bias voltage of 500 μV is applied to each graphene DQD device. The transport current is then amplified by a current preamplifier (SR570) with a bandwidth of 100 Hz. Both the noise of the individual device and the cross-correlation of the two cavity-connected devices are measured in the frequency domain by using the dynamic signal analyzer with a sampling rate of 102.4 kHz and a span of 125 mHz to 100 Hz (see the Supporting Information). The normalized zero-frequency cross-current spectrum $F_{12} = S_{12}(0)/(\langle I_{DQD1}\rangle\langle I_{DQD2}\rangle)^{1/2}$, in the absence of the cavity driving field, is shown in Figure 4c. Here the signal $S_{12}(0)$ was averaged over ten measurements before taken out from the DSA. The signal of $S_{12}(0)$ is in the order of 10^{-27} A^2/Hz. The F_{12} can be converted to the noise power spectrum density by a factor of 10^{-24} A^2/Hz (see the Supporting Information). With the detuning of DQD1 fixed around $\varepsilon_1 \sim hf_0$ (and $\varepsilon_1 \sim 0$), we measured F_{12} as a function of the detuning ε_2 across three different charge transitions of DQD2 with typical $2t_{C2}$ values. The result is shown in Figure 4c. A single broad peak is observed in F_{12} for $2t_{C2} > hf_0$, while two additional side-peaks appear around $\Omega_2 = hf_0$ (where the DQD2 is in resonance with the resonator) for $2t_{C2} < hf_0$.

Based on previous theoretical work,[9] we calculate the normalized cross-current noise spectrum F_{12} using the method of full counting statistics[34] with QuTiP,[35] and with the parameters obtained from a separate fitting process.[18] Figure 4d shows the simulation results corresponding to Figure 4c. The peak positions in the experimental data are qualitatively consistent with the simulations (see the black dashed lines in Figure 4c,d). In addition, for $2t_{C2} = 4.3$ GHz, there is an extra peak around $\varepsilon_2 = -1$ GHz (see red dashed line in Figure 4c) compared to the corresponding simulation, which we cannot explain with the present model. To be noted, the center peak in Figure 4c may be caused by $1/f$ noise[32,33] or steady current correlations; however, the side peaks can only be induced by a novel cross-correlations between the two DQDs.[9−12] (See the Supporting Information for details.)

Moreover, if we apply large microwave power into the resonator, F_{12} shows a triple-peak structure (Figure 4e,f), where the two side peaks are around $\varepsilon_2 = \pm hf_0$, which may be due to a photon-assisted tunneling (PAT) effect that is activated when the resonator is driven by a strong driving field.

Our measurements demonstrate a positive cross-current correlation through the two DQDs. Similar cross-current correlation measurements have been reported in two capacitively coupled quantum dots,[36] in two-particle Aharonov−Bohm interferometer,[37] and in Cooper-pair devices.[38] In these experiments, the correlated electron sources are coupled directly via Coulomb interaction,[36,37] or the correlated electrons originate from the splitting of Cooper pairs.[38] In contrast, there is no significant direct coupling between the electron sources in our device, where instead the DQDs only interact indirectly via the superconducting resonator. One can understand this nonlocal interaction as follows: DQD1 emits an excitation (real or virtual photon) into the resonator,[20] which can be absorbed by DQD2 near its resonance with the resonator ($\Omega_2 \sim hf_0$). The result is that the currents through two DQDs are correlated (Figure 4a,b), which has been argued by theoretic works to be important to entangle distant nanoconductors and may be used for the Bell test.[9−12]

Though there is still a long way to go before reaching the strong-coupling[2] regime (coupling strength larger than the decoherence rates) in a DQD-resonator hybrid system, the large coupling strength (tens of MHz) opens up the possibility to study the interaction between two distant qubits made of quantum dot circuits. Compared to previous work on SQDs,[17] our DQD-based devices offer tunable two-level systems with energy scales closer to the resonator resonance, making it easier to reach the photon-DQD resonance condition.

Due to the Klein tunneling in graphene, it is difficult to consistently obtain interdot tunnel rates below the resonator frequency.[18,25,39] In our device, only DQD2 can satisfy the resonance condition under typical gate voltages. DQD1 cannot be tuned into resonance because its tunnel coupling is larger than the photon energy throughout our investigated area. As a result, we can only tune the current through DQD1 by DQD2, but not the other way around. To study two DQDs both in resonance with the resonator, a resonator with larger resonance frequency would be needed. In addition, graphene could also be replaced by GaAs,[14,16] carbon nanotube,[13,17] or InAs nanowire[15,20] systems.

Conclusions. Two graphene double quantum dots separated by a distance of about 60 μm are coupled to a half-wavelength reflection-line resonator. Resonator amplitude readout results show a dip near the DQD charge-degeneracy point, which can be described by the T−C model. This result demonstrates that the two distant DQDs simultaneously interact with one microwave mode, which can be valuable for the future long-distance interactions between quantum-dot-based qubits. In addition, the correlation between the currents of these two DQDs is studied by measuring the cross-current correlations. The device and the interaction demonstrated here may provide an avenue for exploring nonlocal electronic transport and correlation, although achieving a resonator-mediated coherent interaction between quantum-dot-based

DOI: 10.1021/acs.nanolett.5b02400
Nano Lett. 2015, 15, 6620−6625

qubits would require quantum dots with significantly longer coherence times.

■ ASSOCIATED CONTENT

Supporting Information

The Supporting Information is available free of charge on the ACS Publications website at DOI: 10.1021/acs.nanolett.5b02400.

Further information on sample fabrication and measurement setup, the transport properties, T−C model (PDF)

■ AUTHOR INFORMATION

Corresponding Author

*E-mail: gpguo@ustc.edu.cn.

Author Contributions

G.-W.D. and D.W. contributed equally to this work.

Notes

The authors declare no competing financial interest.

■ ACKNOWLEDGMENTS

We thank M.R. Delbecq and Klaus Ensslin for fruitful discussions. This work was supported by the National Fundamental Research Programme (Grant No. 2011CBA00200), the National Natural Science Foundation (Grant Nos. 11222438, 11174267, 11274294, 61306150, 11304301, and 91121014), and the Chinese Academy of Sciences.

■ REFERENCES

(1) Raimond, J. M.; Brune, M.; Haroche, S. *Rev. Mod. Phys.* **2001**, *73* (3), 565−582.

(2) Wallraff, A.; Schuster, D. I.; Blais, A.; Frunzio, L.; Huang, R. S.; Majer, J.; Kumar, S.; Girvin, S. M.; Schoelkopf, R. J. *Nature* **2004**, *431* (7005), 162−167.

(3) You, J. Q.; Nori, F. *Nature* **2011**, *474* (7353), 589−97.

(4) Xiang, Z.-L.; Ashhab, S.; You, J. Q.; Nori, F. *Rev. Mod. Phys.* **2013**, *85* (2), 623−653.

(5) Childress, L.; Sørensen, A.; Lukin, M. *Phys. Rev. A: At., Mol., Opt. Phys.* **2004**, *69* (4), 042302.

(6) Guo, G.-P.; Zhang, H.; Hu, Y.; Tu, T.; Guo, G.-C. *Phys. Rev. A: At., Mol., Opt. Phys.* **2008**, *78* (2), 020302.

(7) Lin, Z.-R.; Guo, G.-P.; Tu, T.; Zhu, F.-Y.; Guo, G.-C. *Phys. Rev. Lett.* **2008**, *101* (23), 230501.

(8) Hu, X. D.; Liu, Y. X.; Nori, F. *Phys. Rev. B: Condens. Matter Mater. Phys.* **2012**, *86* (3), 035314.

(9) Lambert, N.; Flindt, C.; Nori, F. *EPL (Europhysics Letters)* **2013**, *103* (1), 17005.

(10) Contreras-Pulido, L. D.; Emary, C.; Brandes, T.; Aguado, R. *New J. Phys.* **2013**, *15* (9), 095008.

(11) Bergenfeldt, C.; Samuelsson, P. *Phys. Rev. B: Condens. Matter Mater. Phys.* **2013**, *87* (19), 195427.

(12) Bergenfeldt, C.; Samuelsson, P.; Sothmann, B.; Flindt, C.; Buettiker, M. *Phys. Rev. Lett.* **2014**, *112* (7), 076803.

(13) Delbecq, M. R.; Schmitt, V.; Parmentier, F. D.; Roch, N.; Viennot, J. J.; Fève, G.; Huard, B.; Mora, C.; Cottet, A.; Kontos, T. *Phys. Rev. Lett.* **2011**, *107* (25), 256804.

(14) Frey, T.; Leek, P. J.; Beck, M.; Blais, A.; Ihn, T.; Ensslin, K.; Wallraff, A. *Phys. Rev. Lett.* **2012**, *108* (4), 046807.

(15) Petersson, K. D.; McFaul, L. W.; Schroer, M. D.; Jung, M.; Taylor, J. M.; Houck, A. A.; Petta, J. R. *Nature* **2012**, *490* (7420), 380−3.

(16) Toida, H.; Nakajima, T.; Komiyama, S. *Phys. Rev. Lett.* **2013**, *110* (6), 066802.

(17) Delbecq, M. R.; Bruhat, L. E.; Viennot, J. J.; Datta, S.; Cottet, A.; Kontos, T. *Nat. Commun.* **2013**, *4*, 1400.

(18) Deng, G.-W.; Wei, D.; Johansson, J. R.; Zhang, M.-L.; Li, S.-X.; Li, H.-O.; Cao, G.; Xiao, M.; Tu, T.; Guo, G.-C.; Jiang, H.-W.; Franco, N.; Guo, G.-P. *arXiv*: 1310.6118, **2013**.

(19) Viennot, J. J.; Delbecq, M. R.; Dartiailh, M. C.; Cottet, A.; Kontos, T. *Phys. Rev. B: Condens. Matter Mater. Phys.* **2014**, *89* (16), 165404.

(20) Liu, Y.-Y.; Petersson, K. D.; Stehlik, J.; Taylor, J. M.; Petta, J. R. *Phys. Rev. Lett.* **2014**, *113*, 036801.

(21) Liu, Y. Y.; Stehlik, J.; Eichler, C.; Gullans, M. J.; Taylor, J. M.; Petta, J. R. *Science* **2015**, *347* (6219), 285−287.

(22) Viennot, J. J.; Dartiailh, M. C.; Cottet, A.; Kontos, T. *Science* **2015**, *349* (6246), 408−411.

(23) Tavis, M.; Cummings, F. W. *Phys. Rev.* **1968**, *170* (2), 379.

(24) Wang, L.-J.; Cao, G.; Tu, T.; Li, H.-O.; Zhou, C.; Hao, X.-J.; Su, Z.; Guo, G.-C.; Jiang, H.-W.; Guo, G.-P. *Appl. Phys. Lett.* **2010**, *97* (26), 262113.

(25) Wei, D.; Li, H.-O.; Cao, G.; Luo, G.; Zheng, Z.-X.; Tu, T.; Xiao, M.; Guo, G.-C.; Jiang, H.-W.; Guo, G.-P. *Sci. Rep.* **2013**, *3*, 3175.

(26) Manucharyan, V. E.; Koch, J.; Glazman, L. I.; Devoret, M. H. *Science* **2009**, *326* (5949), 113−116.

(27) Zhang, M.-L.; Deng, G.-W.; Li, S.-X.; Li, H.-O.; Cao, G.; Tu, T.; Xiao, M.; Guo, G.-C.; Jiang, H.-W.; Siddiqi, I.; Guo, G.-P. *Appl. Phys. Lett.* **2014**, *104* (8), 083511.

(28) Majer, J.; Chow, J. M.; Gambetta, J. M.; Koch, J.; Johnson, B. R.; Schreier, J. A.; Frunzio, L.; Schuster, D. I.; Houck, A. A.; Wallraff, A.; Blais, A.; Devoret, M. H.; Girvin, S. M.; Schoelkopf, R. J. *Nature* **2007**, *449* (7161), 443−7.

(29) Xu, C. R.; Vavilov, M. G. *Phys. Rev. B: Condens. Matter Mater. Phys.* **2013**, *87* (3), 035429.

(30) Frey, T.; Leek, P. J.; Beck, M.; Ensslin, K.; Wallraff, A.; Ihn, T. *Appl. Phys. Lett.* **2011**, *98* (26), 262105.

(31) Konstantatos, G.; Badioli, M.; Gaudreau, L.; Osmond, J.; Bernechea, M.; de Arquer, F. P. G.; Gatti, F.; Koppens, F. H. L. *Nat. Nanotechnol.* **2012**, *7* (6), 363−368.

(32) Li, H.-O.; Cao, G.; Xiao, M.; You, J.; Wei, D.; Tu, T.; Guo, G.-C.; Jiang, H.-W.; Guo, G.-P. *J. Appl. Phys.* **2014**, *116* (17), 174504.

(33) Song, X. X.; Li, H. O.; You, J.; Han, T. Y.; Cao, G.; Tu, T.; Xiao, M.; Guo, G. C.; Jiang, H. W.; Guo, G. P. *Sci. Rep.* **2015**, *5*, 8142.

(34) Flindt, C.; Novotny, T.; Jauho, A. P. *EPL (Europhysics Letters)* **2005**, *69* (3), 475−481.

(35) Johansson, J. R.; Nation, P. D.; Nori, F. *Comput. Phys. Commun.* **2013**, *184* (4), 1234−1240.

(36) McClure, D. T.; DiCarlo, L.; Zhang, Y.; Engel, H. A.; Marcus, C. M.; Hanson, M. P.; Gossard, A. C. *Phys. Rev. Lett.* **2007**, *98* (5), 056801.

(37) Neder, I.; Ofek, N.; Chung, Y.; Heiblum, M.; Mahalu, D.; Umansky, V. *Nature* **2007**, *448* (7151), 333−337.

(38) Wei, J. A.; Chandrasekhar, V. *Nat. Phys.* **2010**, *6* (7), 494−498.

(39) Raith, M.; Ertler, C.; Stano, P.; Wimmer, M.; Fabian, J. *Phys. Rev. B: Condens. Matter Mater. Phys.* **2014**, *89*, 085414.

DOI: 10.1021/acs.nanolett.5b02400
Nano Lett. 2015, 15, 6620−6625